Published in final edited form as:
Chem Res Toxicol. 2012 December 17; 25(12): 2642–2653. doi:10.1021/tx3002753.

Reaction of Human Cytochrome P450 3A4 with Peroxynitrite: Nitrotyrosine Formation on the Proximal Side Impairs its Interaction with NADPH-Cytochrome P450 Reductase

Hsia-lien Lin[§], **Cesar Kenaan**[§], **Haoming Zhang**[§], and **Paul F. Hollenberg**[*]
Department of Pharmacology, University of Michigan, Ann Arbor, Michigan

Abstract

The reaction of peroxynitrite (PN) with purified human cytochrome P450 3A4 (CYP3A4) resulted in the loss of the reduced-CO difference spectrum, but the absolute absorption spectrum of the heme was not significantly altered. The loss of 7-benzyloxy-4-(trifluoromethyl)coumarin (BFC) *O*-debenzylation activity of CYP3A4 was concentration dependent with respect to PN and the loss of BFC activity supported by NADPH-cytochrome P450 reductase (CPR) was much greater than that supported by *tert*-butyl hydroperoxide. Moreover, the PN-treated CYP3A4 exhibited a reduced-CO spectrum when reduced by CPR that was much smaller than when it was reduced by dithionite. These results suggest that modification of CYP3A4 by PN may impair its interaction with CPR leading to the loss of catalytic activity. Tyrosine nitration, as measured by an increase in mass of 45 Da due to the addition of a nitro group, was used as a biomarker for protein modification by PN. PN-treated CYP3A4 was digested by trypsin and endoproteinase Glu C, and nitrotyrosine formation was then determined by using electrospray ionization-liquid chromatography-tandem mass spectrometry. Tyr residues 99, 307, 347, 430 and 432 were found to be nitrated. Using the GRAMM-X docking program, the structure for the CYP3A4-CPR complex shows that Tyr99, Tyr347 and Tyr430 are on the proximal side of CYP3A4 and are in close contact with three acidic residues in the FMN domain of CPR, suggesting that modification of one or more of these tyrosine residues by PN may influence CPR binding or the transfer of electrons to CYP3A4. Mutagenesis of Tyr430 to Phe or Val revealed that both the aromatic and hydroxyl groups of Tyr are required for CPR-dependent catalytic activity and thus support the idea that the proximal side Tyr participates in the 3A4-CPR interaction. In conclusion, modification of tyrosine residues by PN and their subsequent identification can be used to enhance our knowledge of the structure/function relationships of the P450s with respect to the electron transfer steps which are critical for P450 activity.

Introduction

Peroxynitrite (PN)[1], a potent oxidant and nitrating agent, is generated from the reaction of nitric oxide and superoxide in an almost diffusion-controlled reaction under

[*]To whom correspondence should be addressed: Paul F. Hollenberg, Department of Pharmacology, 2301 MSRB III, 1150 West Medical Center Drive, Ann Arbor, MI 48109-5632, Phone: (734) 764-8166. Fax: (734) 763-5387. phollen@umich.edu.
[§]These authors contributed equally to this paper.

Supporting Information **Available:**
The PDB file for the GRAMM-X CYP3A4-CPR complex is available free of charge via the internet at http://pubs.acs.org.

[1]**Abbreviations**
CYP3A4, human cytochrome P450 3A4; CPR, NADPH-cytochrome P450 reductase; PN, peroxynitrite; ESI-LC-MS/MS, electrospray ionization-liquid chromatography-tandem mass spectrometry; BFC, 7-benzyloxy-4-(trifluoromethyl)coumarin, BHP, *tert*-butyl hydroperoxide; Glu C, endoproteinase Glu C; WT 3A4, wild type or untreated CYP3A4; Y430F mutant, 3A4 in which Tyr430 has been mutated to Phe; Y430V mutant, 3A4 in which Tyr430 has been mutated to Val.

pathophysiological conditions. The formation of nitrotyrosines in vivo represents a specific PN-mediated protein modification; thus, the detection of nitrotyrosine in proteins is considered to be a biomarker for endogenous formation of PN (1). PN formation is proposed to contribute to a number of diseases including cerebral ischemia, cardiovascular diseases, and neurodegenerative disorders (2). The addition of a nitro group to Tyr results in the following: (a) the p*K*a of the tyrosine hydroxyl group decreases by 2-3 units, causing the Tyr to be partially charged at physiological pHs and to be more hydrophilic in its local environment; and (b) the addition of a bulky nitro moiety may disrupt hydrogen bonding between the hydroxyl group of tyrosine and nearby residues, thereby disrupting the structural integrity of the protein, and potentially resulting in steric hinderance of substrate access to the active site or disrupting protein-protein interactions (3-5). Thus, nitration of tyrosine may result in perturbations in enzymatic activity through distortion of the active site or impairment of electron transfer from CPR to a P450.

The selectivity for PN-mediated formation of nitrotyrosine is residue-, protein-, and tissue-specific (6-8). However, not all of the tyrosines modified by nitration will necessarily affect protein function. For example, peroxynitrite reacts with both the Mn and Cu,Zn superoxide dismutases to form nitrotyrosine; however, while the Mn superoxide dismutase was inactivated, the Cu,Zn superoxide dismutase was not affected (9). The mechanism of tyrosine nitration by PN was originally thought to proceed via a free radical pathway, but under *in vivo* physiological conditions, the presence of a carbonyl group or metal ions seems to play a dominant role in the sensitivity and selectivity of tyrosine nitration. Specifically, the reaction of PN with heme-thiolate containing proteins was found to be facilitated by the formation of ferryl intermediates, thus explaining why P450s, which are heme-thiolate proteins, are nitrated with high efficiency (1, 10).

The rat microsomal cytochrome P450 3A subfamily is able to catalyze the oxidation of N-hydroxyarginine and other C=N(OH) bond-containing compounds leading to the formation of nitric oxide (11). The physiological formation of nitric oxide during inflammatory responses by cytochrome P450 3A has also been documented (12). The generation of excess superoxide resulting from electron uncoupling in mitochondrial electron transport, NADPH-oxidase activity, or uncoupled catalytic turnover during the P450 catalytic cycle can ultimately lead to reaction of the superoxide anion with nitric oxide to form PN. Therefore, it is likely that PN can be generated in the vicinity of the P450 3A subfamily of proteins and that P450 3A could potentially be a target for modification by PN (13).

A key step in the P450 catalytic cycle involves the transfer of electrons from its redox partner, NADPH-cytochrome P450 reductase (CPR). The prerequisite step for the transfer of electrons is the formation of a complex between the hemoprotein and the flavoprotein. A co-crystal structure of P450 and CPR is not available yet and many questions regarding the nature of the interaction and the mechanism by which the electrons are transferred remain to be answered. Among the mammalian P450s, the majority of studies on P450-CPR interactions have been concerned with the CYP2B4-CPR interactions (14-16), whereas the interaction between human cytochrome P450 3A4 (CYP3A4) and its redox partner, CPR, has not been well characterized (17-18). By comparing the *tert*-butyl hydroperoxide (BHP)- and CPR-dependent catalytic activities, previous studies have suggested that PN-mediated protein modification impairs the interaction between CPR and P450s 2B1, 2B6 and 2E1 (19-20). However, the region(s) on the proteins involved in binding and the identities of the contact residues between P450 and CPR have not been determined. These previous results along with the availability of a user friendly web interface for the GRAMM-X program have led us to investigate whether PN could be used as a chemical probe to detect the site of interaction of CPR with CYP3A4 (21).

CYP3A4, the most abundant cytochrome P450 in human liver, metabolizes a wide range of endogenous and exogenous compounds and is believed to be responsible for the metabolism of more than 60% of all clinically relevant drugs (22). Thus, it would be of great interest to investigate the effect of PN on the structure and function of human CYP3A4. Therefore, in this study, CYP3A4 was treated with various concentrations of PN and the decreases in the catalytic activity supported by either NADPH/CPR or BHP were compared. PN-modified CYP3A4 was digested with trypsin and/or endoproteinase Glu C (Glu C) and analyzed by electrospray ionization-liquid chromatography-tandem mass spectrometry (ESI-LC-MS/MS). The mass shift which results from the addition of a nitro group (45 Da) by PN was used to identify the sites of modification of the Tyr residues by using the SEQUEST database search as described previously (23). The addition of PN to CYP3A4 resulted in a concentration-dependent loss of catalytic activity that was much greater for the reaction supported by CPR than for that supported by BHP. The differential effect on the loss of catalytic activity supported by CPR compared to BHP suggested that PN-mediated nitration of residues Tyr99, Tyr347 and Tyr430 on the proximal surface of CYP3A4 impaired the interaction of the CYP3A4 with CPR. Using the GRAMM-X docking program, a model structure of the complex of CYP3A4 with CPR was constructed to facilitate the interpretation of the experimental results and mutagenesis studies were then performed in order to test the model.

Materials and Methods

Materials

PN was purchased from Cayman Chemicals (Ann Arbor, MI) and stored at −80°C prior to use. 7-Benzyloxy-4-(trifluoromethyl)coumarin (BFC) was from BD Biosciences (Franklin Lakes, NJ). NADPH, BHP, Glu C, L-α-dilauroyl-phosphocholine, L-α-dioleyl-*sn*-glycero-3-phosphocholine, and L-α-phosphatidylserine were from Sigma-Aldrich Chemical Co. (St. Louis, MO). Sequencing grade modified trypsin was from Promega (Madison, WI). All other chemicals and solvents used were of the highest purity available from commercial sources.

Site-directed Mutagenesis

The human CYP3A4 plasmid was used as a template to construct two mutant proteins at position Tyr430. The mutations were carried out using the in vitro QuickChange site-directed mutagenesis kit (Stratagene Products, Agilent Technologies, Santa Clara, CA). The primer 5′-GGACAACATAGATCCTTTCATATACACACCCTTTGG-3′ was used for the Tyr430 to Phe conversion (Y430F mutant). The primer 5′-GGACAACATAGATCCTGTCATATACACACCCTTTGG-3′ was used for the Tyr to Val conversion (Y430V mutant). The mutations were confirmed by DNA sequencing carried out at the University of Michigan Biomedical Core Facility (Ann Arbor, MI).

Purification of Enzymes and Determinations of Enzymatic Activities

The wild type CYP3A4 (WT), the Y430F mutant and the Y430V mutant were expressed in their N-terminal truncated and His-tagged C-terminal forms in *E. coli* TOPP3 cells and the proteins were purified to homogeneity using methods we have previously described (20). CPR was expressed and purified according to methods previously described (20). CYP3A4 (1 nmol) was reconstituted with 60 μg of a mixture of L-α-dilauroyl-phosphocholine, L-α-dioleyl-*sn*-glycero-3-phosphocholine, and L-α-phosphatidylserine (1:1:1) in 1 ml of 100 mM potassium phosphate buffer, pH 7.7 and then treated with various concentrations of PN (9.4, 18.8, 37.5, 75, 150, and 300 μM) at room temperature for 5 min. The control and PN-treated CYP3A4 samples were treated identically and then assayed for catalytic activity using the following two methods. For the BHP-supported catalytic activity, the 7-

benzyloxy-4-(trifluoromethyl)coumarin (BFC) *O*-debenzylation activity was determined in 100 mM potassium phosphate buffer (pH 7.7) containing 50 μM BFC, 25 mM BHP and 60 pmol of CYP3A4 by incubation at room temperature for 15 min. For the CPR-supported activity, 20 pmol of CYP3A4 were reconstituted with 60 pmol of CPR for 30 min at 37 °C and the activity remaining was determined using an assay mixture containing 50 μM BFC and 200 μM NADPH in a final volume of 250 μl in 100 mM potassium phosphate buffer, pH 7.7. The catalytic activity of all the PN-treated samples was compared to the control sample that was not exposed to PN as previously described (20). PN decays in a few seconds under physiological conditions, thus excluding the possibility that CPR would be modified in the assays used to determine activity remaining after treatment with PN for 5 min (24).

Spectral Analysis

The absorbance spectra of the heme in the control and PN-treated samples (0.4-0.6 nmol) were determined by scanning from 400-600 nm on a UV-Vis 2501 PC spectrophotometer at room temperature (Shimadzu Corporation, Kyoto, Japan). The maximal absorbance at ~418 nm was used to determine heme content (19). The reduced CO difference spectra of the P450s were determined as described by Omura and Sato (25). Control and PN-modified P450s were reduced by the addition of CPR (1.5 nmol) and NADPH (0.5 mM) in the presence of 200 μM testosterone and then bubbled with CO until no further changes in the spectra were observed. Sodium dithionite (~1 mg) was then added and additional scans were performed until no further changes were observed.

Trypsin and Glu C Digestion of the Modified P450

500 pmol of untreated P450 or P450 treated with 300 μM PN was denatured by incubation with 6M urea at 60 °C for 45 min followed by exchanging the buffer with 100 mM ammonium bicarbonate (pH 8.0) and concentrated using Amicon Ultra centrifuge filter devices with a 10,000 Da MW cutoff (Millipore Corporation, Billerica, MA). Aliquots (100 μl) of the concentrated samples were digested with 2 μg trypsin and/or Glu C at 37 °C for 18 h. The digested peptide solutions were centrifuged at 16,000 × g and the clear supernatants were subjected to LC-MS/MS analysis.

LC-MS/MS Analysis of the Digested Proteins

A C18 reversed phase column (Jupiter, 5 μm, 2.0 × 100 mm, Phenomenex, Torrance, CA) was used to analyze the digested samples. The mobile phase consisted of solvent A (0.05% formic acid and 0.05% TFA in water) and solvent B (0.05% formic acid and 0.05% TFA in acetonitrile). The initial gradient was 10 to 25% B for 10 min followed by a linear gradient to 65% B over 35 min and then increasing linearly to 95% B over 10 min at a flow rate of 0.3 ml/min on a Shimadzu LC-10AD system (Kyoto, Japan). The column effluent was directed into an LCQ Deca XP mass spectrometer (Thermo Fisher Scientific). The electrospray ionization conditions are: sheath gas flow rate, 60 arbitrary units; auxiliary gas, 10 arbitrary units; spray voltage, 4.5 kV; capillary voltage, 30V; capillary temperature 220 °C; and tube lens offset, 60 V. Data were acquired in positive mode using Xcalibur software (Thermo Fisher Scientific) in a data-dependent experiment where MS/MS data were collected on the six most abundant ions in the survey scan.

Identification of Tyr Residues Modified by PN

The observed peptide masses were exported to the SEQUEST dataset software in BioWorks 3.3.1 as previously described (23). The addition of a nitro group to a tyrosine residue will increase the residue's mass by 45 Da, thus the modification of a Tyr in a peptide by PN would be expected to result in a mass shift of 45 Da. The predicted enzymatic full mass spectrum and fragmentation to give the b and y ions of the tryptic peptides was obtained

using the ProteinProspector (http://prospector.ucsf.edu/) computer program. The MS/MS spectra of the modified peptides were further analyzed with Xcalibur software and compared with the theoretical fragmentations of the modified peptides to confirm the peptide sequence and the identity of the residue modified by PN.

Modeling of the interaction of CYP3A4 and CPR

The docking of CYP3A4 and CPR was performed using the GRAMM-X public web server at http://vakser.bioinformatics.ku.edu/resources/gramm/grammx/ (21). The crystal structure of CYP3A4 (PDB file 1TQN) (26) and CPR in an open conformation (PDB file 3ES9) (15) were submitted to GRAMM-X as the ligand and receptor, respectively. The crystal structure of a genetically engineered CPR in an open conformation revealed three different conformations (Mol A, B, and C) (15). The most ordered of the three open conformations is Mol A. In the GRAMM-X docking parameters, chain ID A was designated as the amino acid chain for both the receptor and ligand structures. Although Mol A is the most ordered conformation, it is important to note that Mol A likely represents only a single conformation of the active form of CPR and that other open conformations may exist in solution. Asp208 of CPR was provided as a potential receptor residue and Arg130 of CYP3A4 was provided as a potential ligand residue. Our rationale for selecting these residues was the following. The role of Asp208 in CPR has been studied extensively by Shen and Kasper (27) who found that when mutated to Asn it gave the single largest perturbation of the P450 dependent benzphetamine *N*-demethylase activity and it was also recently used in the GRAMM-X docking of CYP2B4 and CPR (15). With regards to the selection of a residue in CYP3A4, previous studies have shown that several basic, solvent-exposed and evolutionary conserved residues within the 2B subfamily located on the proximal surface of 2B4 are involved in binding CPR (14). However, very few studies have been performed to characterize the kinetics of electron transfer between CPR and CYP3A4 and to determine the identity of specific 3A4 residues in CYP3A4 that bind CPR (17-18, 28-29). Aligning the amino acid sequences of CYP2B4 (a P450 isoform that has been well characterized in terms of its interaction with CPR) and CYP3A4 showed that Arg130 in 3A4 was highly conserved among many mammalian P450s including 1A2, 2B1, 2B4, 2B6, 2C9, 3A4 and 3A5. Arg130 in CYP3A4 corresponds to Arg125 in CYP2B which has been proposed to bind b_5 (30) and CPR (31) and located in the overlapping binding region of CPR and b_5 (14). Therefore, on the basis that a CYP3A4 residue which binds CPR would most likely be positively charged, conserved and solvent-exposed, Arg130 in CYP3A4 was chosen as it fulfills all these criteria.

Results

The Effect of PN on the Heme Content, the Reduced-CO Spectrum, and Catalytic Activity of CYP3A4

When CYP3A4 was treated with various concentrations of PN (9-300 μM), the absolute absorbance of the heme prosthetic group was not significantly altered, but the reduced-CO spectrum of the CYP3A4 chemically reduced by dithionite decreased significantly in a concentration-dependent manner (Fig. 1). Following exposure of CYP3A4 to various concentrations of PN, the BHP- or CPR-supported catalytic activities were determined and the data are reported as % activity remaining relative to untreated CYP3A4 (100% control). As shown in Fig. 1, PN-treated CYP3A4 exhibits a concentration-dependent loss in BFC catalytic activity. At a PN concentration higher than 37 μM, the loss of activity supported by CPR is much greater than that supported by BHP.

Comparison of P450 Reduced-CO Spectra of CYP3A4 Following Reduction by CPR and Dithionite

As shown in Fig. 2c, the reduced-CO difference spectrum of CYP3A4 that had been exposed to 150 μM PN and then reduced enzymatically by CPR and NADPH is ~10% of that of the control that had not been exposed to PN (Fig. 2a). Because there was no significant loss of heme after treatment with PN (data not shown), the results suggest that PN-modified CYP3A4 apoprotein has lost either some of its ability to accept electrons from CPR or its ability to bind CPR leading to the decrease observed in the reduced-CO spectrum. Following the addition of dithionite, the amount of reduced-CO complex was recorded again. The reduced-CO spectrum of the untreated CYP3A4 following reduction by dithionite increased ~10% (Fig. 2b versus Fig. 2a), while the addition of dithionite to the PN-treated CYP3A4 resulted in a significant increase in the reduced-CO spectrum (Fig. 2d versus Fig. 2c). It appears that the transfer of the first electron from NADPH by CPR to the heme iron in PN-treated CYP3A4 is severely impaired. Moreover, the decrease in the extent of the spectrum formation at 450 nm and the emergence of the peak at 420 nm after the treatment of PN, as shown in Fig. 2d, suggested that the heme-thiolate ligation is partially destroyed.

LC-MS/MS Analysis of Peptides Modified by Reaction with PN

PN-treated CYP3A4 was digested with trypsin and/or Glu C and then analyzed by LC-MS/MS as described in Materials and Methods. The modification of Tyr by the addition of a nitro group would be expected to result in a mass shift of 45 Da (NO_2 minus H). A SEQUEST search using this mass indicated four modified peptides (Table 1). The MS/MS spectra of the modified peptides were further analyzed using Xcalibur software and compared with the theoretical fragmentations predicted for the modified peptide using ProteinProspector software to confirm the modified peptide sequences and the identities of the residues modified by PN (23). The nitration of Tyr99 (shown in Fig. 3), Tyr307 (shown in Fig. 4) and Tyr347 (shown in Fig. 5) was confirmed from the MS/MS spectra of the singly charged precursor ions at *m/z* 1163.4, 1616.6 and 1410.5, respectively. Nitration of both Tyr430 and Tyr432 was confirmed from the MS/MS spectrum of the doubly charged precursor ion having a *m/z* 951.6 (shown in Fig. 6). The predicted b and y ions for the PN-modified peptides were calculated from the unmodified peptide with an increase of 45 Da on the Tyr residue by using ProteinProspector software and displayed in the top panel of each modified peptide. Shown in red are the observed b and y ions for the modified peptides. Some of the fragments observed are from the loss of H_2O or NH_3 (Figures 3-5), and some of the fragments observed are doubly charged (Fig. 6). In general, almost all of the b and y ions can be assigned in each of the modified peptides. In short, Tyr residues at position 99, 307, 347, 430 and 432 of CYP3A4 were identified to be nitrated by exposure to PN under the conditions described. We have identified four peptides containing five nitrated tyrosines out of a total of 14 tyrosines in CYP3A4. Some of the nitrated Tyr may have escaped detection by LC-MS/MS analysis or the SEQUEST database search. Moreover, Cys239 was oxidized by PN as identified by a mass increase of 48 Da (data not shown). Therefore, we cannot rule out that modification of residues other than the Tyrs by PN may contribute to the loss of CYP3A4 catalytic activity. After CYP3A4 was treated with PN, the mass of apoprotein was analyzed by LC-MS. The mass increases of the apoprotein were 92, 101, 149, and 298 Da for PN concentrations of 37, 75, 150, and 300 μM, respectively. Thus the PN-mediated mass increases correlate well with the losses in catalytic activity.

Location of the Nitrated Tyrosines and their Surrounding Residues in the CYP3A4 Crystal Structure

The crystal structure of CYP3A4 at 2.05 Å resolution (26) serves as an excellent resource to determine the potential intra-protein effects of tyrosine nitration by PN and may help in

understanding the physical and chemical factors that determine the selectivity for tyrosine nitration. Tyr99, Tyr430, Tyr432 and Tyr347 are located approximately 15 Å away from the heme iron while Tyr307 is approximately 8 Å away. With the exception of Tyr307, all of the nitrated tyrosines are located in the proximal side of CYP3A4. The locations of the Tyr residues with respect to the overall structure of CYP3A4 and the locations and the identities of the residues within 4.5 Å of each of the Tyr residues are shown in Fig. 7. In general, the nitrated tyrosines are located either in loops or at the C-terminal end of a loop (e.g. Tyr347) and are surrounded by hydrophobic and basic residues. Specifically, the benzene ring of Tyr99 is within ~4 Å of Trp126, Pro439 and Lys127 and may interact with these surrounding residues via van der Waals interactions. Tyr430 is similarly surrounded by hydrophobic residues as it is within ~4 Å of Pro429, Lys91, Val95 and Ser437. Tyr430's benzene ring can form van der Waals interactions with the β- and γ-carbons of Pro429, the β-, γ-, and δ-carbons of Lys91 and the γ_1- or γ_2-carbons of Val95. Similarly, Tyr432 forms a series of intermolecular interactions that may be important in maintaining the tertiary structure of CYP3A4. With regard to hydrophobic interactions, the benzene ring of Tyr432 forms van der Waals interactions with the γ- and δ-carbons of Pro434 as well as π-stacking interactions with the benzene rings of Phe419. In addition, the hydroxyl group of the phenol ring of Tyr432 is located within hydrogen-bonding distance of the carbonyl group of Asn361. The benzene ring of Tyr347 can form van der Waals interactions with Leu142 and Leu351 as well as with the β-, γ-, and δ-carbons of Lys143. Furthermore, the hydroxyl group of Tyr347 can form hydrogen bond with the carbonyl group of Arg446. Lastly, the benzene ring of Tyr307 can form van der Waals interactions with Leu211 and Ilu184 while the hydroxyl group can form hydrogen bond with the amine group of Lys208. From these observations it is clear that all of the nitrated tyrosine residues form significant numbers of hydrophobic and hydrogen bonding interactions. Since these interactions may serve to maintain the preferred tertiary structure of CYP3A4, their perturbation due to nitration of these tyrosines by PN may lead to a loss of the three dimensional protein structural integrity and enzymatic activity.

Modeling of the binding of CPR to CYP3A4

The GRAMM-X docking program has been used by numerous laboratories to determine model structures of protein-protein complexes in the past (21). Very recently a public web server version of GRAMM-X was made available which, along with the recent crystal structure of a genetically engineered CPR in an open conformation capable of reducing P450, enabled the docking of CYP3A4 with CPR (15). In this docking model, Arg130 in CYP3A4 as a ligand is 4 Å away from Asp208 as a receptor in CPR and the two residues can form a salt-bridge with each other. Our model for the formation of the CYP3A4-CPR complex reveals several details regarding the interaction of the tyrosines of CYP3A4 with residues located in the FMN domain of CPR. First, in order to assess the validity of our docking results, we compared our model to the results of Hamdane et al. (15) which were conducted for docking CYP2B4 to CPR using the same docking program. Since the majority of the mutagenic studies aimed at identifying the residues which dictate P450-CPR binding have focused on the basic residues of CYP2B4 and very little is known with respect to which residues in CYP3A4 are involved in binding CPR, we performed a sequence alignment of CYP2B4 with CYP3A4 to determine if some of the residues in CYP2B4 believed to bind CPR are also conserved in CYP3A4. From a list of six basic charged residues (Arg122, Arg126, Arg133, Lys139, Arg422 and Lys433) identified by Bridges et al. (14) to play roles in the binding to CPR, the basic residue in CYP2B4 that is conserved between CYP2B4 and CYP3A4 is Arg122, which corresponds to Lys127 in CYP3A4. The model reveals that Lys127 is 4.6 Å away from Glu213 in CPR and thus the two residues would be capable of forming a salt-bridge with each other. Glu213 is part of a cluster of acidic residues in CPR involved in interactions between cytochrome P450 and cytochrome c

(27). Furthermore, Arg130 of CYP3A4, which is conserved among most mammalian P450s, is within hydrogen bonding distance of Thr88 in CPR. To further test the validity of our model we looked at whether the residues in CPR reported to bind with CYP2B4 might also be forming intermolecular interactions with CYP3A4. Hamdane et al. (15) showed that the interface of the CYP2B4-CPR model consists of residues Glu92, Glu93, Asp113, Glu142 and Asp208 of the FMN domain of CPR which form salt-bridges with their basic counterparts Arg122, Arg126, Lys433, Arg422 and Arg133, respectively, in CYP2B4. In our CYP3A4-CPR model, Glu92 is 2.3 Å away from Tyr430, Glu93 is 5.6 Å away from Tyr99, and Glu142 is 6.8 Å away from Tyr347 (Fig. 8A). The hydrogen bonding between Asp208 in CPR and Ser134 in 3A4 is 3 Å while Asp113 does not interact with any CYP3A4 residues. Therefore, the majority of the nitrated proximal surface tyrosine residues may form hydrogen bonds or are in close contact with glutamic acid residues in the FMN domain of CPR and contribute partially to formation of the CYP3A4-CPR complex. Compared to the untreated CYP3A4, the enzymatic reduction of CYP3A4 by NADPH/CPR was severely impaired by PN treatment whereas reduction by dithionite showed a significant (about 5-fold) increase over the CPR-dependent reduction (Fig. 2). Therefore, it is likely that nitration of residues Tyr99, Tyr347 and Tyr430 by PN impairs the interaction of CYP3A4 with CPR. This may be achieved directly by inhibiting the interaction of Tyr99, Tyr347 and Tyr430 with CPR and/or indirectly by perturbing the interaction of neighboring CYP3A4 residues with CPR. To better visualize the interface between CYP3A4 and CPR, the prosthetic heme of CYP3A4 and the FMN of CPR have been superimposed on the corresponding chains in the GRAMM-X model. The distance between the heme and the FMN domain is 10.7 Å. The location of the three Tyr residues of CYP3A4 and the three Glu residues of CPR relative to the heme and the FMN domain are shown in Fig. 8B. It appears that Glu142 faces the 7,8-dimethylisoalloxazine moiety while Glu92 and Glu93 face the 5′-phosphoric ester tail.

Mutagenesis Studies of Y430F and Y430V Mutants

Since our model for the formation of the CYP3A4-CPR complex revealed that the Tyr430 in CYP3A4 participates in hydrogen bonding with Glu92 in CPR with a distance between the two residues of 2.3 Å, Tyr430 was chosen for further mutagenesis studies. The reduced-CO spectrum of the P450 reduced by CPR and then further reduced by the addition of dithionite was determined for WT 3A4 as well as Y430F and Y430V mutants. The results shown in Fig. 9 indicate that the reduced-CO spectrum of WT 3A4 reduced by CPR did not change significantly (from “a” to “b”) upon addition of dithionite while the Y430F mutant increase by 2-fold (from “c” to “d”) and the Y430V mutant increased by greater than 4-fold (from “e” to “f”) upon addition of dithionite. It is clear that CPR can only partially support the formation of reduced-CO complex with these two variants when compared to WT 3A4. In addition, the BFC debenzylation activity of the WT and the two mutants supported by BHP and CPR was investigated. The relative P450-CO spectra formed by NADPH/CPR versus that formed by dithionite (as 100%) for each P450 and the relative catalytic activities of the mutant P450s compared to WT 3A4 (as 100%) were analyzed. As summarized in Table 2, the percentage of the CPR-dependent P450-CO spectrum compared to the dithionite reduced P450-CO spectrum is 88, 41, and 22% for WT 3A4, the Y430F mutant, and the Y430V mutant, respectively, suggesting that the two mutants lose some of their ability to accept electrons from CPR for the formation of the reduced P450-CO spectrum when compared to WT 3A4. Furthermore, the CPR-dependent catalytic activity of the CYP3A4 mutants is markedly suppressed compared to WT 3A4, with only 40% and 10% activities observed for the Y430F and Y430V mutants, respectively; but the BHP-dependent catalytic activity still exhibits 87% and 70% of the WT activity for the Y430F and Y430V mutants, respectively. These results suggest that the replacement of Tyr by Phe or Val impaired the interaction between CYP3A4 and CPR and that the presence of the hydroxyl group is of greater importance for complex formation than the aromatic moiety.

Discussion

We have reported the inhibitory effect of PN on CYP3A4 and characterized the formation of nitrotyrosine as a marker for protein modification by PN. After the exposure of CYP3A4 to PN, the absolute absorption spectrum of the heme was not significantly altered, but the reduced P450-CO spectrum decreased significantly with the emergence of a peak at 420 nm. It appears that PN modification of amino acid residues alters the coordination of the heme with the cysteine axial ligand and perturbs the heme-thiolate ligation. After CYP3A4 was treated with various concentrations of PN, the BHP-dependent BFC *O*-debenzylation catalytic activity remaining correlated well with the remaining P450-CO spectrum reduced by dithionite. However, at PN concentrations higher than 37 μM, the CPR-dependent, but not the BHP-dependent, catalytic activity decreased dramatically, suggesting that PN modified certain residues resulting in alterations in the formation of the CYP3A4-CPR complex. When the level of the reduced P450-CO spectrum formed with NADPH/CPR was compared to that obtained after adding dithionite, the P450-CO spectrum of the PN-treated CYP3A4 reduced with dithionite was significantly increased, but that was not observed for the untreated CYP3A4. These results indicate that almost all the reduced P450-CO spectrum can be observed with NADPH/CPR for the untreated CYP3A4, but not the PN-treated CYP3A4. Since the PN-treated CYP3A4 was reduced by NADPH/CPR to a significantly lesser extent than the untreated CYP3A4, it appears that the transfer of the first electron from NADPH via CPR to the heme iron in CYP3A4 is impaired following treatment with PN.

The results shown in Fig. 1 and Fig. 2 indicate clearly that apoprotein modification is the major contributor for the loss of CYP3A4 catalytic activity. The most stable product of PN attack on proteins results from the addition of a nitro group to the C3 position of Tyr to form 3-nitrotyrosine. This modification can be detected by immunological techniques or by LC-MS/MS analysis by determining the increase in the mass of protein of 45 Da on the digested peptide (2, 5). The detection of 3-nitrotyrosine in proteins has been utilized as a biomarker for the *in vivo* formation of PN in the pathogenesis of disease (7). Here, we focus on the characterization of the effect of this modification of tyrosine on CYP3A4's structure and function. Five tyrosine residues: Tyr99, Tyr307, Tyr347, Tyr430 and Tyr432, were found to be nitrated by PN by using LC-MS/MS analysis.

Previous studies have demonstrated that the formation of complexes between P450s and their redox partners occurs on the proximal side of P450s and on the FMN domain region of CPR and that the intermolecular electrostatic interactions play a major role in complex formation (14-15, 27). However, depending on the identities of the surface residues of the individual P450s, non-charged attractions including hydrophobic and intermolecular hydrogen bonding interactions have also been suggested to be dominant factors in stabilizing the binding of the hemoprotein to the flavoprotein (16, 32-34). Thus, by comparing the differential effect of PN on P450 reduction to give the reduced P450-CO spectrum by NADPH/CPR to that by dithionite as well as the differential effect of PN on the BHP- and CPR-dependent catalytic activities, we concluded that nitrotyrosine formation on the proximal side of CYP3A4 impairs its interaction with CPR. Since very little is known regarding the structural basis of CYP3A4's interaction with its redox partner, GRAMM-X was used to virtually dock CYP3A4 to CPR in order to better understand the potential physical and chemical roles of surface exposed tyrosines of CYP3A4 in mediating protein-protein interactions. In this docking experiment, the 2.05 Å crystal structure of CYP3A4 (1TQN) was docked to the 3.4 Å crystal structure of CPR (3ES9) in an open conformation (shown to be the active form of CPR). The docking model revealed a series of potential direct and indirect effects that the reaction of PN with tyrosines on CYP3A4 would have on the formation of the CYP3A4-CPR complex. Specifically, of the five tyrosines which were

identified by LC-MS/MS analysis of the proteolytically digested PN-modified 3A4, Tyr99, Tyr347 and Tyr430 were 5.6 Å away from Glu93, 6.8 Å away from Glu142, and 2.3 Å away from Glu92 in CPR, respectively. A previous GRAMM-X-generated model of the complex between CYP2B4 and Mol A of CPR revealed that the contacts between the two proteins are mostly electrostatic in nature and are defined by five possible salt bridges (Glu92, Glu93, Asp113, Glu142, and Asp208 from the FMN domain and five positive residues of CYP2B4) (15). The present CYP3A4-CPR complex model shows that three of the modified Tyr residues, Tyr99, Tyr347 and Tyr430 are in close proximity to three of the acidic residues of CPR, Glu93, Glu142 and Glu92, respectively (Fig. 8). Therefore, based on the virtual docking results, it appears that CYP3A4 and CYP2B4 share a similar contact region in CPR. However, which intermolecular interactions contribute the most to complex formation may be dictated by the individual surface residues on the P450 (34). For example, the CYP3A4-CPR docking model shows that the hydroxyl group of Tyr430 forms a hydrogen bond with the carbonyl group of Glu92 in the FMN domain of CPR with a distance of 2.3 Å. Tyrosine is an aromatic residue whose side chain contains a hydroxyl and benzene group, the addition of a bulky nitro group at the C3 position in tyrosine due to reaction with PN may reduce the *p*Ka of its phenolic OH from ~10 to ~7.5, causing the normally hydrophobic tyrosine to be partially charged and more hydrophilic in the local environment (3-5). The deprotonation of the hydroxyl group of the phenol moiety in nitrotyrosine may disrupt the hydrogen bond network and result in some loss in the structural integrity of protein. The bulky nitro group may also cause a conformational change or some steric hindrance in CYP3A4. All of these changes have the potential to perturb intermolecular interactions between these Tyr residues or the residues nearby and their counterparts on CPR, thus impairing the formation of the CYP3A4-CPR complex.

The prevailing notion in the field regarding the interaction of P450 with CPR is that a series of basic residues on the proximal side of P450 form salt bridges with a cluster of acidic residues in the FMN domain of CPR (14-15, 27). Therefore, the interface between CYP3A4 and CPR in the complex likely contains not only tyrosine residues from CYP3A4, but lysines and arginines as well. For example, as shown in Figure 7, Tyr99 is in close proximity to Lys127, which our docking model revealed was 4.8 Å away from the Glu213 of CPR. Tyr347 is surrounded by two basic residues, Lys143 and Arg446, which are 5.5 Å and 5.8 Å away from Glu142 and Asp147 in CPR, respectively. Additionally, Tyr430 is close to Lys91, which is 3.0 Å away from Glu92 and Tyr84 in CPR. Since the benzene rings of Tyr99, Tyr347 and Tyr430 form hydrophobic interactions with the saturated aliphatic carbons of their neighboring lysine and arginine residues, the addition of a nitro group to produce nitrotyrosine could conceivably perturb the hydrophobic interactions of the three nitrated tyrosines with their lysine/arginine neighbors and indirectly impair binding to acidic residues in CPR. Therefore, it is likely that the nitration of tyrosines on the proximal side of CYP3A4 hinders functional binding to CPR by interfering directly with the intermolecular interactions between the tyrosines in CYP3A4 and the glutamic residues in CPR or indirectly by perturbing the interactions of surrounding lysine/arginine residues in CYP3A4 with residues in CPR.

The photoaffinity ligand lapachenole has been shown to covalently modify Cys98 of CYP3A4. This adduct formation led to the loss of CYP3A4 catalytic activity and further mutagenesis studies suggested that substitution of an aromatic residue at position 98 triggered a critical conformational change which affected the interaction of P450 with CPR by decreasing the binding affinity of P450 for its redox partner (17, 35). Tyr99 is located next to Cys98 and the side chains of the two residues are relatively close to each other, as shown in Fig. 7. Given the previously identified role of Cys98 and the proximity of this residue to Tyr99, a possible explanation for our observed results is that the formation of the nitrotyrosine at position 99 may lead to structural changes in the local environment of Tyr99

leading to steric interference of the interaction between CYP3A4 and CPR. Similarly, nitrotyrosine formation on Tyr347 and Tyr430 may potentially trigger either structural changes in CYP3A4 or may interfere directly with the association of CPR and 3A4 by sterically interfering with the intermolecular interactions.

Unlike what we previously observed with CYP2B1, CYP2B6, and CYP2E1 (20, 36), the conversion of the reduced P450-CO spectrum to its inactive P420 form following exposure of CYP3A4 to PN indicates that heme-thiolate ligation was altered. A noticeable difference between the CYP2 P450s and CYP3A4 is that not all the residues modified by PN in CYP3A4 are surface exposed. For instance, Tyr307, located in the I-helix, is found in substrate recognition site 4 and is ~8 Å away from heme center. It is likely that nitration of this residue may crowd the active site or induce conformational changes in the heme environment, and thus affect CO binding to the ferrous heme and decrease the catalytic activity as well. Additionally, Tyr432, which is surrounded by several hydrophobic residues, is located on the proximal side and its side chain faces toward the heme-Cys442 region. Thus, modification of this residue is likely to change the heme-iron ligation required for the optimal reduced-CO binding spectrum and/or disrupt the proper structure for the ligation of the heme iron with the axial cysteine ligand required for activity.

To test our hypothesis that the proximal side residues such as Tyr99, Tyr347 and Tyr430 may be involved in the interaction with CPR, Tyr430 was replaced by Phe or Val using site-specific mutagenesis and the two variants were expressed and purified. The results show that the P450 reduced-CO spectrum reduced by CPR is less than 50% that produced by reduction with dithionite of both of the variants. Moreover, replacement of the Tyr with Phe or Val decreases the CPR-dependent activity to a much greater extent than the BHP-dependent catalytic activity. All of these results indicate that the transfer of the first electron from NADPH via CPR to the two mutants is severely impaired. These results from the mutagenesis of Tyr430 correlate well with the effect of PN on CYP3A4. The formation of nitrotyrosine as a result of exposure to PN not only disrupts hydrogen bonding, but can also produce an unfavorable hydrophilic environment (5). The possibility that the tyrosine hydroxyl group can act as a potential hydrogen bond acceptor/donor while the benzene ring can form hydrophobic interactions has been demonstrated during the transfer of electrons from formate dehydrogenase to the Tyr64 of cytochrome c_{553} (37). Whether hydrogen bonding, hydrophobic interactions of the Tyr, or the positive residues in the immediate vicinity of Tyr play a dominant role in the formation of the CYP3A4-CPR complex remains to be investigated.

In conclusion, nitration of the tyrosine residues on the proximal side of CYP3A4 by PN leads to the loss of catalytic activity through the impairment of CYP3A4-CPR interactions. Chemical modification of Tyr residues of CYP3A4 by PN can be a useful tool for studying the role of specific residue(s) in the electron transfer process from CPR to P450. Although the function of tyrosine residues in mediating the interaction between CPR and several mammalian P450s including CYPs 1A2, 2B1, 2B6, and 2E1 has been addressed, the identities of the contact residues between the P450s and the FMN domain of CPR have not yet been characterized (19-20, 38). Here, on the basis of GRAMM-X docking of CYP3A4 to CPR, the functional and structural role of residue-residue interactions between the two proteins was further investigated to facilitate our understanding of the electron transfer pathways from CPR to the most abundant and most important P450 in human drug metabolism. The generation of PN under inflammatory conditions in the presence of superoxide has the potential to alter drug metabolism by CYP3A4 through the impairment of its catalytic activity by altering the interaction of CYP3A4 with its redox partner. Moreover, the P450s may be responsible for the formation of PN as well as targets for PN-mediated oxidative damage (13). We have previously reported that rat P450 2B1 in rat liver

microsomes was nitrated by PN (19). The formation of nitrotyrosine by P450 *in vivo* has not been reported. However, the detection of 3-nitrotyrosine in human disease has been demonstrated, suggesting that protein tyrosine nitration may be a pathophysiological consequence of various disorders and diseases (1, 8).

Supplementary Material

Refer to Web version on PubMed Central for supplementary material.

Acknowledgments

We thank Dr. Richard Neubig, Department of Pharmacology, University of Michigan (Ann Arbor, MI) for the use of the Wallac Victor II Plate reader.

Funding Sources

This work was supported in part by a grant from the National Institutes of Health [CA-16954].

References

(1). Ischiropoulos H. Biological tyrosine nitration: a pathophysiological function of nitric oxide and reactive oxygen species. Arch. Biochem. Biophys. 1998; 356:1–11. [PubMed: 9681984]

(2). Radi R, Peluffo G, Alvarez MN, Naviliat M, Cayota A. Unraveling peroxynitrite formation in biological systems. Free Radic. Biol. Med. 2001; 30:463–488. [PubMed: 11182518]

(3). Beckman JS, Koppenol WH. Nitric oxide, superoxide, and peroxynitrite: the good, the bad, and the ugly. Am. J. Physiol. 1996; 271:C1424–C1437. [PubMed: 8944624]

(4). Crow JP, Ye YZ, Strong M, Kirk M, Barnes S, Beckman JS. Superoxide dismutase catalyzes nitration of tyrosines by peroxynitrite in the rod and head domains of neurofilament-L. J. Neurochem. 1997; 69:1945–1953. [PubMed: 9349539]

(5). Radi R. Nitric oxide, oxidants, and protein tyrosine nitration. Proc. Natl. Acad. Sci. U. S. A. 2004; 101:4003–4008. [PubMed: 15020765]

(6). Souza JM, Daikhin E, Yudkoff M, Raman CS, Ischiropoulos H. Factors determining the selectivity of protein tyrosine nitration. Arch. Biochem. Biophys. 1999; 371:169–178. [PubMed: 10545203]

(7). Greenacre SAB, Ischiropoulos H. Tyrosine nitration: localisation, quantification, consequences for protein function and signal transduction. Free Radic. Res. 2001; 34:541–581. [PubMed: 11697033]

(8). Turko IV, Murad F. Protein nitration in cardiovascular diseases. Parmacol. Rev. 2002; 54:619–634.

(9). Ischiropoulos H, Zhu L, Chen J, Tsai M, Martin JC, Smith CD, Beckman JS. Peroxynitrite-mediated tyrosine nitration catalyzed by superoxide dismutase. Arch. Biochem. Biophys. 1992; 298:431–437. [PubMed: 1416974]

(10). Daiber A, Bachschmid M, Beckman JS, Munzel T, Ullrich V. The impact of metal catalysis on protein tyrosine nitration by peroxynitrite. Biochem. Biophys. Res. Comm. 2004; 317:873–881. [PubMed: 15081421]

(11). Jousserandot A, Boucher J, Desseaux C, Delaforge M, Mansuy D. Formation of nitrogen oxides including NO from oxidative cleavage of C=N(OH) bonds: a general cytochrome P450-dependent reaction. Bioorg. Med. Chem. Lett. 1995; 5:423–426.

(12). Kuo PC, Abe KY, Dafoe DC. Cytochrome P450IIIA activity and cytokine-mediated synthesis of nitric oxide. Surgery. 1995; 118:310–317. [PubMed: 7543704]

(13). Morgan ET, Ullrich V, Daiber A, Schmidt P, Takaya N, Shoun H, Mcgiff JC, Oyekan A, Hanke CJ, Campbell WB, Park C, Kang J, Yi H, Cha Y, Mansuy D, Boucher J. Cytochrome P450 and flavin monooxygenases-targets and sources of nitric oxide. Drug Metab. Dispos. 2001; 29:1366–1376. [PubMed: 11602511]

(14). Bridges A, Gruenke L, Chang Y, Vakser IA, Loew G, Waskell L. Identification of the binding site on cytochrome P450 2B4 for cytochrome b_5 and cytochrome P450 reductase. J. Biol. Chem. 1998; 273:17036–17049. [PubMed: 9642268]

(15). Hamdane D, Xia C, Im SC, Zhang H, Kim JJ, Waskell L. Structure and function of an NADPH-cytochrome P450 oxidoreductase in an open conformation capable of reducing cytochrome P450. J. Biol. Chem. 2009; 284:11374–11384. [PubMed: 19171935]

(16). Kenaan C, Zhang H, Shea EV, Hollenberg PF. Uncovering the role of hydrophobic residues in cytochrome P450-cytochrome P450 reductase interactions. Biochemistry. 2011; 50:3957–3967. [PubMed: 21462923]

(17). Wen B, Lampe JN, Roberts AG, Atkins WM, Rodrigues AD, Nelson SD. Cysteine 98 in CYP3A4 contributes to conformational integrity required for P450 interaction with CYP reductase. Arch. Biochem. Biophys. 2006; 454:42–54. [PubMed: 16959210]

(18). Farooq Y, Roberts GK. Kinetics of electron transfer between NADPH-cytochrome P450 reductase and cytochrome P450 3A4. Biochem. J. 2010; 432:485–493. [PubMed: 20879989]

(19). Roberts ES, Lin H, Crowley JR, Vuletich JL, Osawa Y, Hollenberg PF. Peroxynitrite-mediated nitration of tyrosine and inactivation of the catalytic activity of cytochrome P450 2B1. Chem. Res. Toxicol. 1998; 11:1067–1074. [PubMed: 9760281]

(20). Lin H, Myshkin E, Waskell L, Hollenberg PF. Peroxynitrite inactivation of human cytochrome P450s 2B6 and 2E1: heme modification and site-specific nitrotyrosine formation. Chem. Res. Toxicol. 2007; 20:1612–1622. [PubMed: 17907788]

(21). Tovchigrenchko A, Vakser IA. GRAMM-X public web server for protein-protein docking. Nucleic Acids Res. 2006; 34:310–314.

(22). Guengerich, FP. Cytochrome P450: Structure, Mechanism, and Biochemistry (Ortiz de Montellano PRed). Plenum Press; New York: 1995. Human Cytochrome P450 enzymes; p. 473-535.

(23). Lin H, Zhang H, Jushchyshyn M, Hollenberg PF. Covalent modification of Thr302 in cytochrome P450 2B1 by the mechanism-based inactivataor 4-tert-butylphenylacetylene. J. Pharmacol. Exp. Ther. 2010; 333:663–669. [PubMed: 20200115]

(24). Daiber A, Herold S, Schoneich C, Namgaladz D, Peterson JA, Ullrich V. Nitration and inactivation of cytochrome P450BM-3 by peroxynitrate: stopped-flow measurements prove ferryl intermediates. Eur. J. Biochem. 2000; 267:6729–6739. [PubMed: 11082183]

(25). Omura T, Sato R. The carbon monoxide-binding pigment of liver microsomes. I. Evidence for its hemoprotein nature. J. Biol. Chem. 1964; 239:2370–2378. [PubMed: 14209971]

(26). Yano JK, Wester MR, Schoch GA, Griffin KJ, Stout CD, Johnson EF. The structure of human microsomal cytochrome P450 3A4 determined by X-ray crystallography to 2.05-Å resolution. J. Biol. Chem. 2004; 279:38091–38094. [PubMed: 15258162]

(27). Shen AL, Kasper CB. Role of Acidic Residues in the interaction of NADPH-cytochrome P450 oxidoreductase with cytochrome P450 and cytochrome c. J. Biol. Chem. 1995; 270:27475–27480. [PubMed: 7499204]

(28). Hlavica P, Schulze J, Lewis DFV. Functional interaction of cytochrome P450 with redox partners: a critical assessment and update of the topology of predicted contact regions. J. Inorg. Biochem. 2003; 96:279–297. [PubMed: 12888264]

(29). Fernando H, Halpert JR, Davydov DR. Kinetics of electron transfer in the complex of cytochrome P450 3A4 with flavin domain of cytochrome P450BM-3 as evidence of functional heterogeneity of heme protein. Arch. Biochem. Biophy. 2008; 471:20–31.

(30). Omata Y, Sakamoto H, Robinson RC, Pincus MR, Friedman FK. Interaction between cytochrome P450 2B1 and cytochrome b_5: inhibition by synthetic peptides indicates a role for P450 residues Lys-122 and Arg-125. Biochem. Biophys. Res. Comm. 1994; 210:1090–1095. [PubMed: 8024550]

(31). Hazai E, Bikadi Z, Simonyi M, Kupfer D. Association of cytochrome P450 enzymes is a determining factor in their catalytic activity. J. Comput. Aided Mol. Des. 2005; 19:271–285. [PubMed: 16163453]

(32). Voznesnsky AI, Schenkman JB. Quantitative analyses of electrostatic interactions between NADPH-cytochrome P450 reductase and cytochrome P450 enzymes. J. Biol. Chem. 1994; 269:15724–15731. [PubMed: 8195225]

(33). Sevrioukova IF, Li H, Zhang H, Peterson JA, Poulos TL. Structure of a cytochrome P450-redox partner electron-transfer complex. Proc. Natl. Acad. Sci. U. S. A. 1999; 96:1863–1868. [PubMed: 10051560]

(34). Sevrioukova IF, Poulos TL. Structural biology of redox partner interactions in P450cam monooxygenase: a fresh look at an old system. Arch. Biochem. Biophys. 2011; 507:66–74. [PubMed: 20816746]

(35). Wen B, Doneanu CE, Gartner CA, Roberts AG, Atkins WM, Nelson SD. Fluorescent photoaffinity labeling of cytochrome P450 3A4 by lapachenol: identification of modification sites by mass spectrometry. Biochemistry. 2005; 44:1833–1845. [PubMed: 15697209]

(36). Lin H, Zhang H, Waskell L, Hollenberg PF. The highly conserved Glu149 and Tyr190 residues contribute to peroxynitrite-mediated nitrotyrosine formation and the catalytic activity of cytochrome P450 2B1. Chem. Res. Toxicol. 2005; 18:1203–1210. [PubMed: 16097793]

(37). Sebban-Kreuzer C, Blackledge M, Dolla A, Marion D, Guerlesquin F. Tyrosine 64 of cytochrome c553 is required for electron exchange with formate dehydrogenase in Desulfovibrio vulgaris Hildenborough. Biochemistry. 1998; 37:8331–8340. [PubMed: 9622485]

(38). Janig GR, Kraft R, Rabe H, Makower A, Ruckpaul K. Comparative studies on the accessibility and functional importance of tyrosine residues in cytochrome P-450 enzymes. Biomed. Biochim. Acta. 1988; 47:565–579. [PubMed: 3202847]

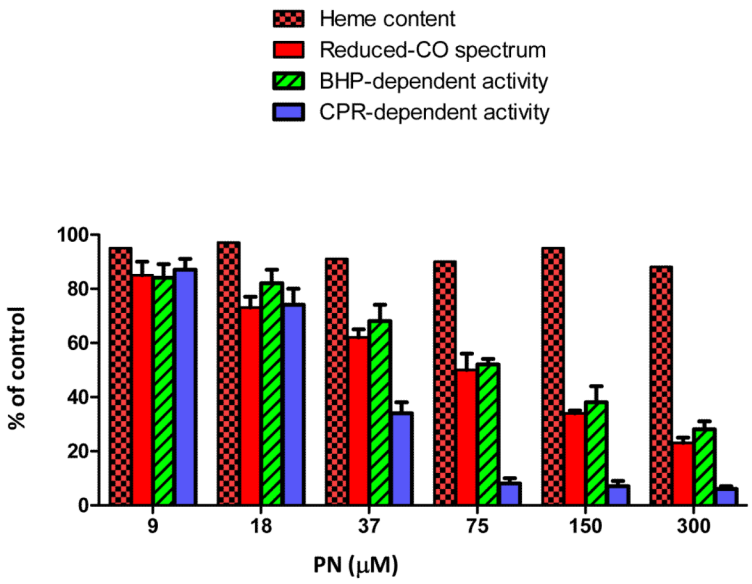

Fig. 1.

Comparison of the heme content, P450-CO spectra reduced by dithionite, BHP-dependent catalytic activity and CPR-dependent catalytic activity of CYP3A4 after reaction with PN. CYP3A4 was treated with PN at the concentrations indicated, and the heme content, the reduced-CO spectra and BFC *O*-debenzylation activity remaining were determined as described in Materials and Methods. The data for the catalytic activities and the reduced P450-CO spectra are from three separate experiments done in duplicate. The data for the heme content are the average of two experiments.

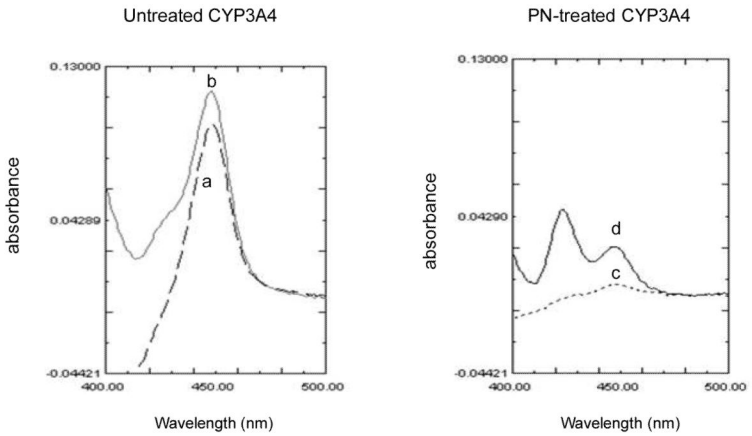

Fig. 2.

Effect of 150 μM PN on the spectrum of the CYP3A4 reduced-CO complex. The reduced P450-CO difference spectra of untreated (a) and PN-treated (c) CYP3A4 were determined after the samples were reconstituted with CPR, testosterone and NADPH and then bubbled with CO as described in Materials and Methods. Spectrum (b) was obtained following the addition of dithionite to (a). Spectrum (d) was obtained following the addition of dithionite to (c).

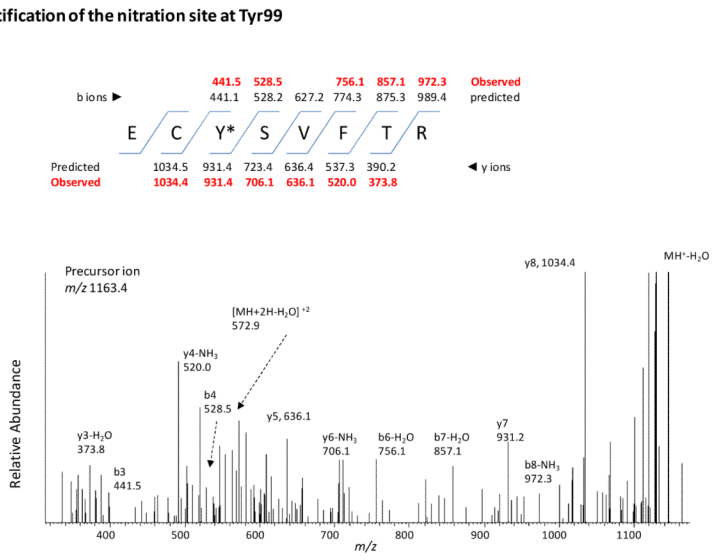

Fig. 3.

LC-MS/MS analysis of the nitrated peptide ^{97}ECYSVFTNR^{105}. The predicted b and y fragment ion series for the singly charged ion with MH^+ at *m/z* 1163.4 for the modified peptide are indicated in the top panel. Data presented are from the MS/MS spectra of the singly charged precursor ion obtained in positive mode using the Xcalibur software. The observed ions for the modified peptide are “shown in red” as described in the text. The modified residue is indicated by the asterisk.

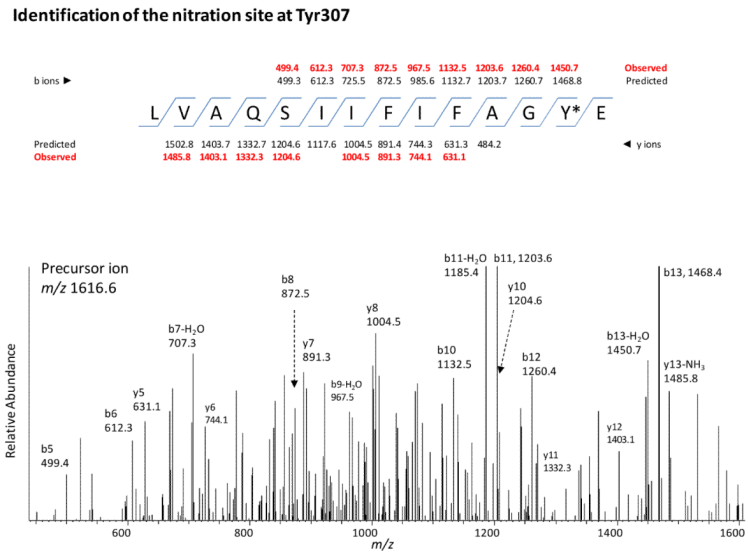

Fig. 4.

LC-MS/MS analysis of the modified peptide ^{295}LVAQSIIFIFAGYE^{308}. The predicted b and y fragment ion series for the singly charged ion with MH^+ at *m/z* 1616.6 for the modified peptide are indicated in the top panel. Data presented are from the MS/MS spectra of the singly charged precursor ion obtained in positive mode using the Xcalibur software. The observed ions for the modified peptide are “shown in red” as described in the text. The modified residue is indicated by the asterisk.

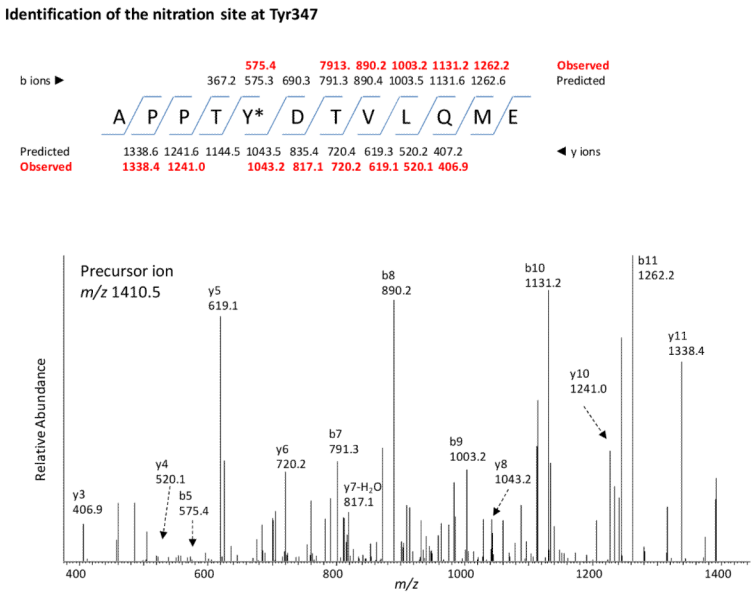

Fig. 5.

LC-MS/MS analysis of the modified peptide ^{343}APPTYDTVLQME^{354}. The predicted b and y fragment ion series for the singly charged ion with MH^+ at *m/z* 1410.5 for the modified peptide are indicated in the top panel. Data presented are from the MS/MS spectra of the singly charged precursor ion obtained in positive mode using the Xcalibur software. The observed ions for the modified peptide are “shown in red” as described in the text. The modified residue is indicated by the asterisk.

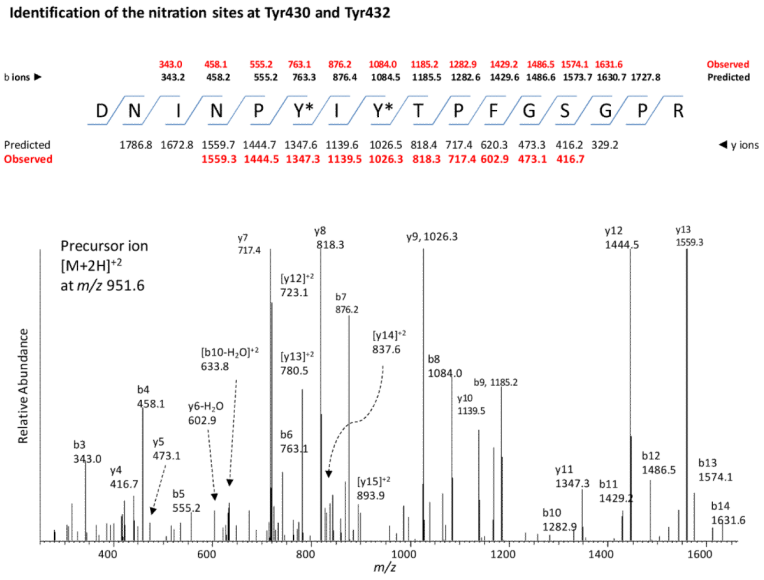

Fig. 6.

LC-MS/MS analysis of the nitrated peptide ^{425}DNIDYIYFGSSPR^{440}. The predicted b and y fragment ion series for the singly charged ion with MH^+ at *m/z* 1903.0 for the modified peptide are indicated in the top panel. Data presented are from the MS/MS spectra of the precursor ion with $[M+2H]^{+2}$ at *m/z* 951.6 obtained in positive mode using the Xcalibur software. The observed ions for the modified peptide are “shown in red” as described in the text. Doubly charged fragment ions y12, y13, y14 and y15 are also observed. The modified residue is indicated by the asterisk.

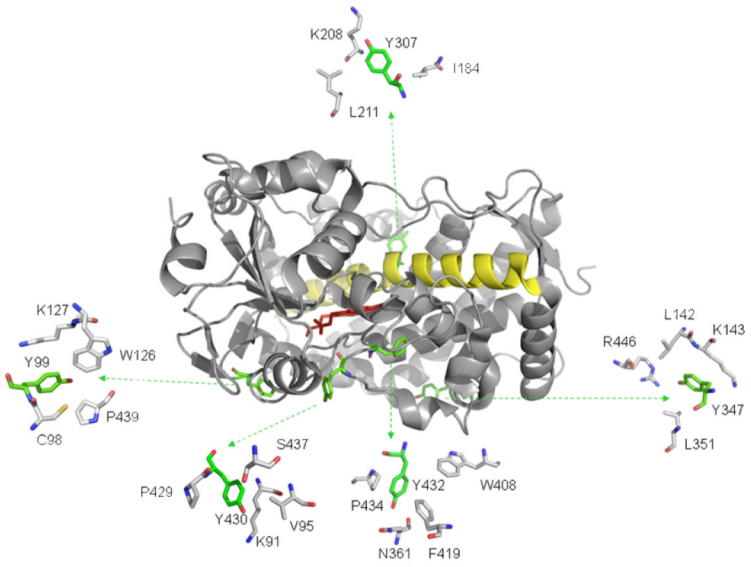

Fig. 7.

The location of nitrated tyrosines in the CYP3A4 crystal structure. Shown in color are the heme (red), I-helix (yellow) and the nitrated tyrosine residues (green). Each of the five nitrated tyrosine residues and the residues within 4.5 Å of them are shown separately for clarity. The potential interaction between the tyrosine residues and neighboring residues are explained in the text. The distances from the heme iron to Y99, Y307, Y347, Y430 and Y432 are 16 Å, 8 Å, 17 Å, 16 Å, and 14 Å, respectively.

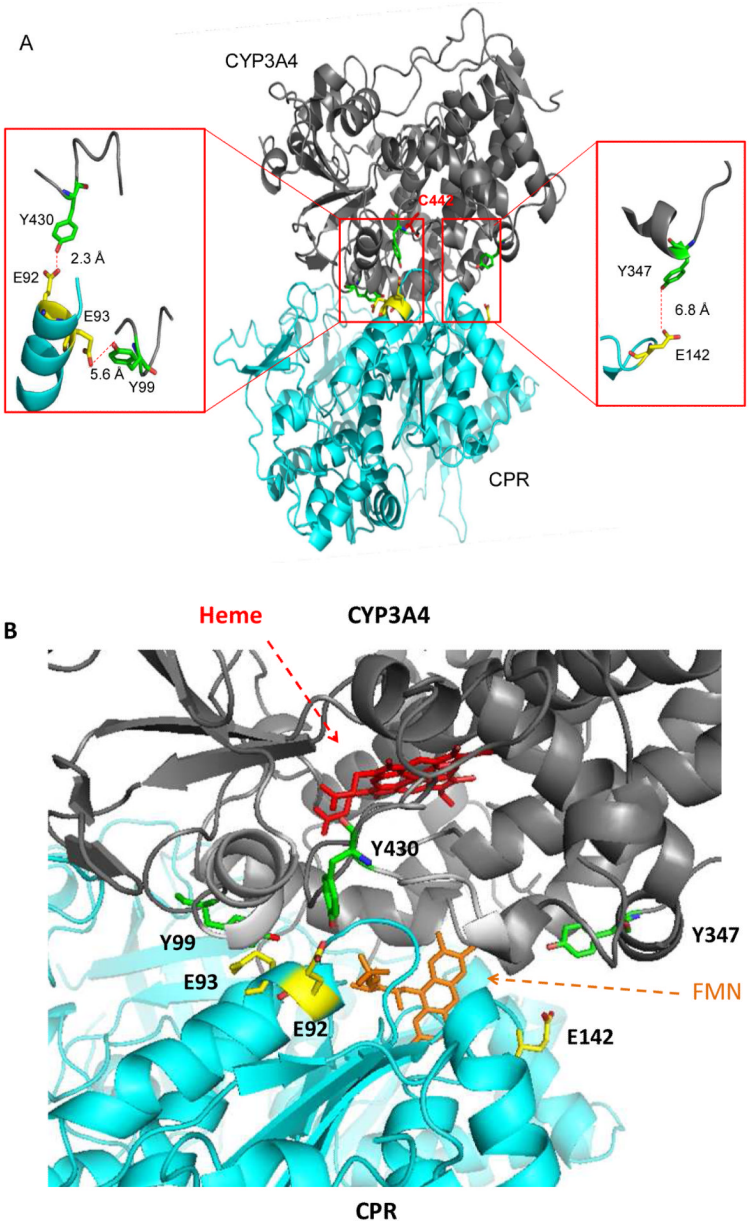

Fig. 8.

GRAMM-X docking model for a complex between CYP3A4 and Mol A of CPR. (A), shown in color are the glutamic acid residues of CPR (yellow), the nitrated tyrosine residues, Y99, Y347 and Y430 of CYP3A4 (green), and the axial ligand to the heme iron, C442 (red). The potential hydrogen bonding interactions between the three nitrated tyrosines of CYP3A4 and the three glutamate residues of CPR are indicated by the red dashed lines and are shown in the expanded view; (B) The heme (in red) and FMN (in orange) from the original crystal structures were superimposed onto the GRAMM-X model for the structure of CYP3A4-CPR. Three Tyr residues of CYP3A4 and three Glu residues of CPR in the interface of CYP3A4-CPR complex are labeled.

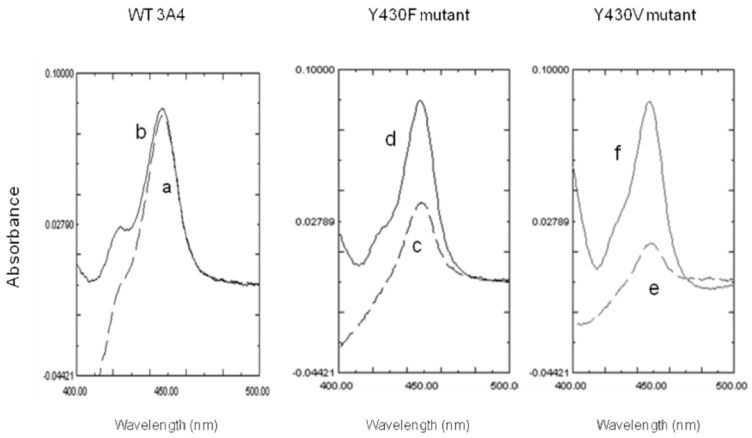

Fig. 9.

Comparison of the P450-CO spectra reduced by NADPH/CPR versus dithionite for WT 3A4 and the Y430F and Y430V mutants. The reduced-CO difference spectra of the three P450s were determined after the samples were reduced by NADPH/CPR and then bubbled with CO (dashed lines a, c and e for WT 3A4, Y430F, and Y430V, respectively). Additional spectra (solid lines b, d, and f for WT 3A4, Y430F, and Y430V, respectively) were obtained following the addition of dithionite as described in Materials and Methods.

Table 1

Summary of the nitrotyrosine-containing peptides identified in PN-treated CYP3A4[a].

Position of nitrated Tyr	Modified peptide sequences	*m/z* of full mass	Precursor ion charge
99	^{97}ECYSVFTNR^{105}	1163.4	1
307	^{295}LVAQSIIFIFAGYE^{308}	1616.6	1
347	^{343}APPTYDTVLQME^{354}	1410.5	1
430 and 432	^{425}DNIDYIYTPFGSSPR^{440}	1903.0	2

[a]PN-treated samples were digested by trypsin and/or Glu C and analyzed by LC-MS/MS as described in Materials and Methods. A mass shift of 45 Da due to nitration of each tyrosine in the peptides analyzed by LC-MS/MS was used for the SEQUEST database search (Lin et al., 2010).

Table 2

Summary of the reduced P450-CO spectra and catalytic activities of WT 3A4 and the Y430F and Y430V mutants.

P450	% of CPR-dependent versus dithionite-dependent reduced P450-CO spectrum	% of relative catalytic activity[a]	
		CPR-dependent	BHP-dependent
WT	88 ± 2	100	100
Y430F	41 ± 3	40 ± 3	87 ± 9
Y430V	22 ± 2	10 ± 1	70 ± 7

[a]The BFC debenzylation activity of the WT3A4 supported by BHP or CPR is designated as 100%. The results presented here were calculated from four separate experiments done in duplicate. The absorbance differences for the reduced-CO difference spectra and the catalytic activities were determined as described in Materials and Methods.